ON THE DESIGN OF THERMALLY LOADED FIBER OPTICS FEEDTHROUGHS

by

***Dragan Z. MARINKOVIĆ*[*a,b], *Manfred W. ZEHN*[b], *and Predrag Dj. MILIĆ*[a]**

[a] Faculty of Mechanical Engineering, University of Nis, Nis, Serbia
[b] TU Berlin, Department of Structural Analysis, Berlin, Germany

Original scientific paper
DOI: 10.2298/TSCI16S5313M

Thermo-mechanical design aspects of various structures exposed to cyclic thermal loading have a crucial impact on their lifetime. This is particularly valid for fiber optics feedthroughs that involve several materials with significantly different thermal expansion ratios. Thermal loading in such structures may give rise to non-trivial thermally induced deformations and therewith stresses, which can be adequately predicted and assessed only by a detailed 3-D numerical simulation. This paper considers a couple of design solutions of fiber optics feedthroughs, which have exhibited certain weaknesses in their application. Numerical simulation by means of the finite element method has been conducted to reveal the weak points of the design.

Key words: *optical fiber feedthrough, finite element method, thermoelasticity*

Introduction

Consideration of thermo-mechanical problems is the key requirement in many engineering applications and has become increasingly important over the past several decades as a consequence of operating conditions of various machines and tools. It is intrinsic for a wide range of problems, such as aerodynamic heating of high speed aircrafts [1], friction heat generation in wheel-rail contact [2], high temperatures generated inside nuclear reactors [3], rapid change in heating in ultra-fast lasers [4], welding [5], to name but a few. In-service environment that involves high temperature changes and temperature gradients that affect the stress state in the considered structures is the common feature of all those problems. Cases where transient thermo-mechanical effects are of importance, such as thermal shocks, cannot be adequately described by the classical thermoelasticity theory that implies infinite speeds of heat conduction. Instead, they call for generalized theories of thermoelasticity such as one developed by Lord and Shulman [6] (often referred as L-S theory). This and similar theories introduce one or more relaxation time parameters into the Fourier heat conduction equation, thus avoiding the paradox of infinite speed of propagation. However, in cases where the steady-states are of primary interest for assessment of thermo-mechanical aspects, *i. e.* the transient behaviour can be neglected, the classical theory of thermoelasticity is sufficient to analyse the problem at hand.

Thermo-mechanical design aspects of fiber optics feedthroughs are in the focus of this paper. Characterization of optical fiber feedtroughs exposed to thermal loads has been al-

* Corresponding author; e-mail: dragan.marinkovic@tu-berlin.de

ready a subject of interest of a number of researchers [7-12]. This paper considers a couple of manufactured designs, which have exhibited severe weaknesses in application, although a simplified 1-D prediction of thermally induced stresses had not pointed out to possible issues. Obviously, the class of problems that admits closed-form solutions in static or dynamic thermoelasticity is evidently small and numerical techniques are inevitably addressed for more complex geometries. Therefore, this study applies the finite element method (FEM) to obtain the detailed 3-D thermal stress field and thus reveal weak points of the design. The computations are based on the classical theory of thermoelasticity.

Classical theory of thermoelasticity and FEM equations

The basic equations of classical linearized thermoelasticity are summarized in this section together with the FEM equations. The balance equations involve the mechanical equilibrium and the heat transfer equation, respectively:

$$\sigma_{ij,j} + \rho f_i = \rho \ddot{u}_i \tag{1}$$

$$\rho T \dot{\eta} = -q_{i,i} + \rho h \tag{2}$$

where superposed dot denotes time derivative, while comma followed by a subscripted index i denotes the partial differentiation with respect to the spatial co-ordinate x_i and the summation convention over the repeated subscripted indices applies. Furthermore, $T = T_0 + \theta$ is the absolute temperature defined by the reference temperature and temperature change.

The constitutive equations yield stresses and entropy, respectively, in the following manner:

$$\sigma_{ij} = C_{ijkl}\varepsilon_{kl} - \beta_{ij}\theta \tag{3}$$

$$\rho\eta = \beta_{ij}\varepsilon_{kl} + \frac{\rho\, c}{T_0}\theta \tag{4}$$

while the heat conduction through a solid is governed by the Fourier's law:

$$q_i = -k_{ij}\theta_{,j} \tag{5}$$

For a proper problem formulation, adequate boundary conditions need to be associated with the previous equations. They may involve prescribed displacements and/or temperatures as well as mechanical (concentrated, surface or volume) loads and/or surface flux acting on certain sub-domains of the considered structure.

The FEM formulation is obtained by the standard procedure, which implies that the primary variables, displacements and temperatures, are related to their nodal values $\{u_e\}$ and $\{\theta_e\}$ by means of adequately chosen shape functions summarized in the matrices $[\mathrm{N}_u]$ and $[\mathrm{N}_\theta]$ for the displacements and temperatures, respectively:

$$\{u\} = [\mathrm{N}_u]\{u_e\}, \qquad \{\theta\} = [\mathrm{N}_\theta]\{\theta_e\} \tag{6}$$

Partial derivatives of the shape functions are required to obtain the strain-displacement matrix, $[\mathrm{B}_u]$ and the temperature gradient matrix $[\mathrm{B}_\theta]$, which in combination with the nodal displacements and temperatures yield strains and temperature gradients, respectively:

$$\{\varepsilon\} = [\mathrm{B}_u]\{u_e\}, \qquad \{\theta'\} = [\mathrm{B}_\theta]\{\theta_e\} \tag{7}$$

The principle of virtual work for the linearized dynamic thermoelasticity reads [13]:

$$\int_V [\delta\{\varepsilon\}^T\{\sigma\} + \delta\theta' q - \delta\theta\rho T_0\dot{\eta}]\mathrm{d}V = \int_V \delta\{u\}^T[\rho\{f\} - \rho\{\ddot{u}\}]\mathrm{d}V +$$

$$+ \int_{A_\sigma} \delta\{u\}^T\{\bar{f}\}\mathrm{d}A_\sigma + \int_{A_q} \delta\theta\bar{Q}\mathrm{d}A_q \tag{8}$$

If the focus is put on a static case, *i. e.* the dynamical effects are neglected and a constant temperature field is assumed, upon substituting the constitutive eqs. (4) and (5) and kinematic relations, eqs. (7), into eq. (8), the resulting FEM system of equations has the form:

$$\begin{bmatrix} \mathrm{K}_{uu} & -\mathrm{K}_{u\theta} \\ 0 & \mathrm{K}_{\theta\theta} \end{bmatrix} \begin{Bmatrix} u_e \\ \theta_e \end{Bmatrix} = \begin{Bmatrix} F_u \\ -F_\theta \end{Bmatrix} \tag{9}$$

where the matrices and vectors are determined in the following manner:

$$[\mathrm{K}_{uu}] = \int_V [\mathrm{B}_u]^T[\mathrm{C}][\mathrm{B}_u]\mathrm{d}V, \quad [\mathrm{K}_{u\theta}] = \int_V [\mathrm{B}_u]^T[\beta][\mathrm{N}_\theta]\mathrm{d}V, \quad [\mathrm{K}_{\theta\theta}] = \int_V [\mathrm{B}_\theta]^T[\mathrm{k}][\mathrm{B}_\theta]\mathrm{d}V,$$

$$\{F_u\} = \int_{A_\sigma} [\mathrm{N}_u]^T\{\bar{f}\}\mathrm{d}A_\sigma, \quad \{F_\theta\} = \int_{A_\theta} [\mathrm{N}_\theta]^T\bar{Q}\mathrm{d}A_\theta \tag{10}$$

The problem considered in this paper implies computation of thermally induced stresses as a consequence of predetermined temperature change. In that case, the predetermined temperature field gives rise to a mechanical load and the system of equations to be solved reads:

$$[\mathrm{K}_{uu}]\{u_e\} = \{F_u\} + [\mathrm{K}_{u\theta}]\{\theta_e\} \tag{11}$$

where the product $[K_{u\theta}]\{\theta_e\}$ yields the thermally induced mechanical loads. Once the nodal displacements are resolved, the kinematic and constitutive relations are used to determine the induced stresses.

Fiber optics feedthroughs exposed to thermal load

In what follows, two designs of fiber optics feedthroughs are considered. Both of them involve four different materials with significantly different thermal expansion ratios. The designs have principally a similar form with a metal shell made of kovar (Ni-Co alloy), which represent the outer layer of the structure. The shell is filled with two different materials – along a part of the length by a solder made of a lead-zinc alloy and the rest of the shell is filled by epoxy glue. In the middle of the shell, along the whole length, there is a glass fiber. The metal shell in both designs has holes due to construction reasons and the later analysis will point out their significance. Figure 1 depicts the both designs in parallel, while figs. 2 and 3 reveal more details about the designs including the dimensions in [mm]. The elastic properties and thermal expansion ratios of all the materials are summarized in tab. 1.

Figure 1. The considered designs of fiber optics feedthroughs

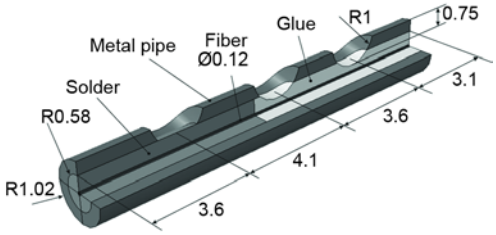

Figure 2. Design A with dimensions in [mm]

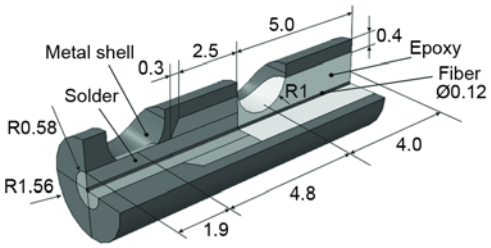

Figure 3. Design B with dimensions in [mm]

Table 1. Material properties

	Young's modulus E, [GPa]	Thermal expansion ratio 10^{-7}[K^{-1}]	Poisson ratio, ν
Glass (fiber)	72.2	5.65	0.26
Kovar (Ni-Co alloy)	140	55.4	0.31
Solder (Pb-Zn alloy)	32.2	268	0.30
Epoxy (glue)	0.81	198	0.41

During the operation the aforementioned fiber feedthroughs are exposed to heat which gives rise to a temperature increase of the whole structure of θ = 120 K compared to the initial, environmental temperature. When the operation is finished, the structures cool down, and this repeats in cycles. In each cycle, the rate of heating and cooling allows to neglect the dynamical effects. If the presence of the holes in the designs was neglected, and by assuming the truss-element kinematics (a cross-section retains its shape and orientation and can only move along the length of the structure), it would be possible to conduct a simple, 1-D computation of thermally induced stresses based on the thermal expansion ratios and Young's moduli of the materials. This is a straightforward exercise and, for the sake of brevity, it is omitted here. Nevertheless, it should be emphasized that based on such a simplified check the considered fiber feedthroughs have been designed and manufactured. However, the first tests have revealed severe issues with the designs, which led to the conclusion that a more detailed analysis was needed.

The FEM models make use of the symmetry, thus modeling one half of the considered structures only. The type of element employed is the quadratic tetrahedral modified thermal analysis element, denoted as C3D10MT in the ABAQUS element library. Upon a convergence analysis, the adopted FEM meshes contain 117409 elements for design A and 105159 elements for design B, fig. 4. One should note that the both FE meshes are more refined in the domain of the glass fiber and its vicinity, as the stress state in the fiber was in the focus of the analysis. As for the boundary conditions, they are specified as a

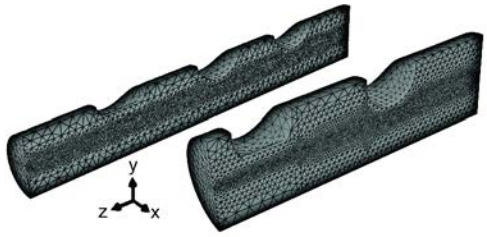

Figure 4. The FEM models: design A – 117409 elements; design B – 105159 elements

constant temperature field of 120 K, while the cross-sections of both designs with the largest z-co-ordinate in fig. 4 were fixed in the z-direction and one node in the middle of the cross-section is completely fixed. A perfect bond is assumed between different materials.

The tests of both designs have shown a significantly shorter lifetime of the fiber than expected. A relatively small number of cycles were sufficient for the cracks to develop in the fiber, which was unexpected based on the aforementioned simplified 1-D check of thermally induced stresses. However, the assessment of the obtained FEM results easily confirms the test results and reveals the weak points in the designs.

Figure 5 shows the FEM results for design A in the vicinity of the middle hole of the metal shell. During heating, the glue expands using the surrounding free space, wherever it can be found, to do so. Due to the relatively large thermal expansion ratio of the epoxy glue and high stiffness of the metal shell, the glue gets pushed out of the metal shell through the hole. This is obvious in the lower part of fig. 5 where the deformation scale factor is set to the value of 3. Such deformational behavior is completely neglected by the simplified 1-D computation. The significantly stiffer solder holds the fiber in place, but at the border between the solder and the glue, the fiber bends towards the hole, as the expanding glue pulls the fiber in that direction. This gives rise to significant stresses on the outer areas of the fiber, particularly in the stretched zone.

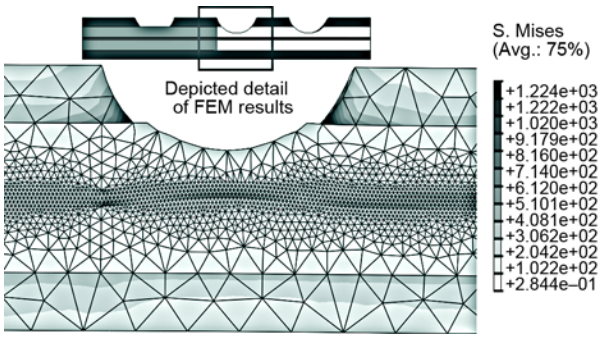

Figure 5. Design A – a side view of the FEM results (deformation scale factor: 3)

The upper part of fig. 6 depicts only a part of the assembly – the deformed solder and fiber, with the deformation scale factor set to the value of 3 so that the fiber bending is visible at the positions corresponding to the two holes of the metal shell. A detail is chosen to show the exact place where fiber leaves the solder and where the stresses in the fiber are maximal due to the bending. The maximal von Mises stress in the fiber yielded by the model exceeds 1200 MPa, but for better understanding of this value, it will be put later in perspective by comparing it with the stress values along the fiber.

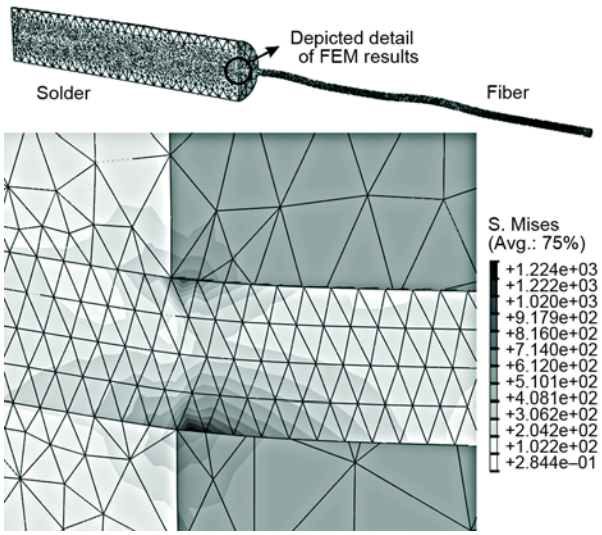

Figure 6. Design A – FEM results for solder and fiber (deformation scale factor: 3)

The same approach used for design A to represent the results is also applied for design B. Figure 7 shows the FEM results in the area starting at the second hole of the metal

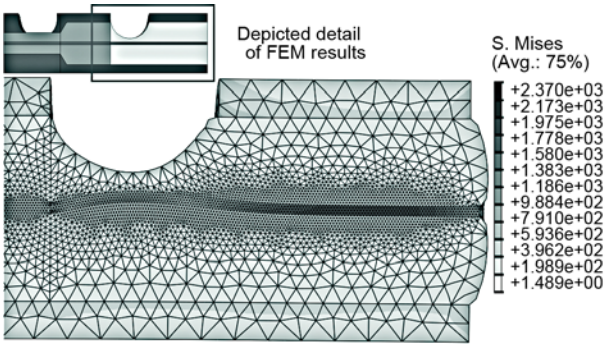

Figure 7. Design B – a side view of the FEM results (deformation scale factor: 3)

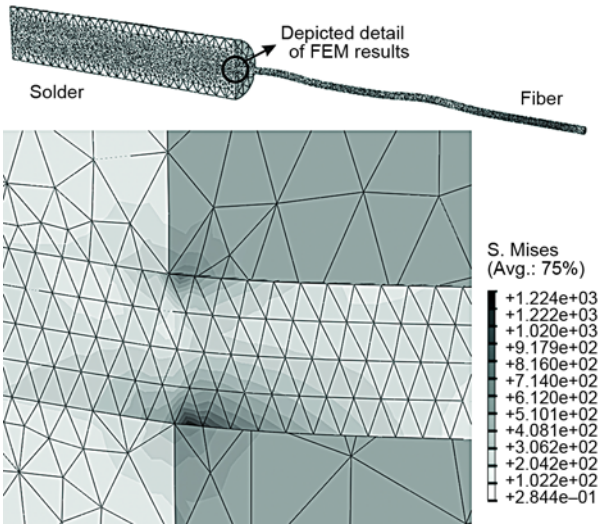

Figure 8. Design A – FEM results for solder and fiber (deformation scale factor: 3)

shell and up to the free end. Also in this case, the deformation scale factor equals 3. The effect of expanding glue is not only visible at the hole, but it is even more obvious at the free end. The deformed configuration reveals that, at the free end, the fiber is exposed to tension in length direction due to the thermally induced expansion of the glue. In that area, it is also exposed to pressure in radial direction, because the stiff metal shell, which has relatively small thermal expansion ratio, hinders the expansion of the glue in radial direction. Nevertheless, as it can be noted in fig. 8, the von Mises stress in the fiber is once again maximal at the position where fiber leaves the solder and bends towards the hole as it is pulled in that direction by the expanding glue. The model yields the value of von Mises stress that exceeds 2300 MPa.

To put the obtained values in perspective, the development of von Mises stress along the fiber is depicted in figs. 9 and 10 for design A and design B, respectively. In both figures, above the diagrams, the deformed fiber is given so that its length corresponds to the horizontal co-ordinate (length of the fiber) in the diagrams. In that manner one can easily associate the stress values from the diagram to their position along the fiber. The stresses are shown along the line on the bottom of the fiber, opposite to the holes, as this is the line along which the maximal stresses in the fiber appear. The diagrams show peaks at the exact positions of transition between the solder and the glue, where the fibers bend towards the hole on the metal shell. This deformational behavior has already been explained above. However, these diagrams show how excessive the stress peaks are, thus exceeding the stress values from those in the rest of the fiber by a large margin. The sharpness of the peaks also points out that the stress values are affected by the singularities in the FEM model caused by the abrupt change in the stiffness in combination with the idealized geometry (perfectly sharp edges) and bond between different materials. Hence, despite the fact that the reliability of the results may be affected by the singularities, the results still demonstrate that this is the area where the maximal stresses occur and that their values are rather high. This assessment was the actual objective of the conducted analysis. The results presented in figs. 9 and 10 confirm the test outcomes that yielded a signifi-

cantly shorter lifetime of the fibers than expected. Cracks were initiated in the fibers exactly at the positions where the stress peaks are seen in these figures.

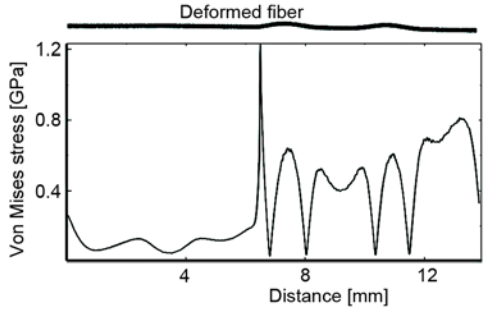

Figure 9. Design A – von Mises stress along the fiber

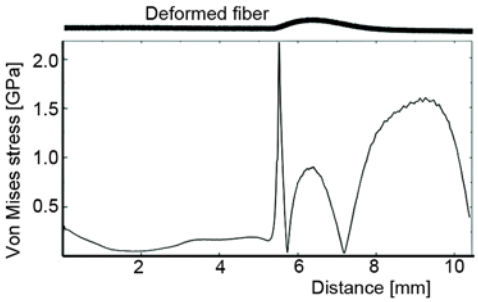

Figure 10. Design B – von Mises stress along the fiber

Conclusions

In their work, engineers tend to simplify the considered problems as much as possible. In doing that, special care is needed in order to retain the important aspects of the problem unaffected by the simplifications. The same is valid for the field of structural analysis. In order to obtain an analytical solution or to keep the FEM solution numerically tractable, it is often of crucial importance to simplify the geometry of the problem. However, oversimplification of the problem may produce misleading results or in Albert Einstein's words "*Everything should be made as simple as possible, but not simpler*". The problem of thermally loaded fiber optics freedthroughs, which are in the focus of this paper, demonstrates this simple principle. As it was shown, the combination of the design, materials with significantly different thermal expansion ratios and thermal loading gives rise to bending of the fiber at the positions corresponding to the holes on the metal shells. This leads to significant stress peaks which cannot be predicted by neglecting the holes in the design with the aim of conducting a simplified computation of thermally induced stresses and, hence, a detailed 3-D FEM analysis was required.

To resolve the presented issue of excessive stress values, one may almost intuitively propose two possible ways. One would be an appropriate change in the design by simply removing the hole from the transition between the solder and the glue, provided such a solution would be constructively acceptable. The fiber bending would still be there, but would also be much smoother and therewith with notably smaller stresses. If a change of the design is not an acceptable solution, one may choose glue with a significantly smaller thermal expansion ratio.

Nomenclature

$[B_u]$ – strain-displacement matrix (FEM), [m^{-1}]
$[B_\theta]$ – temperature gradient matrix (FEM), [m^{-1}]
c – specific heat capacity, [$Jkg^{-1}K^{-1}$]
$[C]$ – Hooke's matrix [Nm^{-2}]
C_{ijkl} – elastic stiffness coefficients, [Nm^{-2}]
fi – body force density, [Nkg^{-1}]
$\{F_u\}$ – nodal forces, [N]
$\{F_\theta\}$ – nodal heat sources, [W]
$\{\bar{f}\}$ – surface traction over the specified boundary surface, [Nm^{-2}]
h – heat source density, [$Jkg^{-1}s^{-1}$]
$[K_{uu}]$ – structural stiffness matrix (FEM), [Nm^{-1}]
$[K_{u\theta}]$ – thermo-mechanical coupling matrix (FEM), [NK^{-1}]
$[K_{\theta\theta}]$ – structural conductivity matrix (FEM), [WK^{-1}]
k_{ij} – thermal conductivity coefficients, [$Wm^{-1}K^{-1}$]
$[k]$ – thermal conductivity matrix, [$Wm^{-1}K^{-1}$]
$[N_u]$ – FE shape functions for displacements (FEM), [–]

$[N_\theta]$ – FE shape functions for temperatures (FEM), [–]
$\bar{Q}$ – heat flux through the specified boundary surface, [Wm^{-2}]
q_i – heat flux, [Wm^{-2}]
T – absolute temperature, [K]
T_0 – reference temperature, [K]
u_i – displacement, [m]
$\{u_e\}$ – nodal displacements (FEM), [m]

Greek symbols

β_{ij} – thermal constants, [NK^{-1}m^{-2}]
$[\beta]$ – thermal matrix, [NK^{-1}m^{-2}]
ε_{kl} – mechanical strains, [–]
η – entropy density, [JK^{-1}kg^{-1}]
θ – temperature change, [K]
$\{\theta_e\}$ – nodal temperature changes (FEM), [K]
$\{\theta'\}$ – temperature gradient, [K/m]
ρ – mass density, [kgm^{-3}]
σ_{ij} – mechanical stresses, [Nm^{-2}]

References

[1] Wu, D., *et al.*, High-Speed and Accurate Calibration of Temperature Sensors for Transient Aerodynamic Heating Experiments, *Transactions of the Institute of Measurement and Control, 36* (2014), 6, pp. 845-852
[2] Miltenović, A., *et al.*, Determination of Friction Heat Generation in Wheel-Rail Contact Using FEM, *Facta Universitatis, series: Mechanical Engineering, 13* (2015), 2, pp. 99-108
[3] Laubscher, R., Dobson, R. T., Theoretical and Experimental Modelling of a Heat Pipe Heat Exchanger for High Temperature Nuclear Reactor Technology, *Applied Thermal Engineering, 61* (2013), 2, pp. 259-267
[4] Mao, Y., Xu, M., Lattice Boltzmann Numerical Analysis of Heat Transfer in Nano-Scale Silicon Films Induced by Ultra-Fast Laser Heating, *International Journal of Thermal Sciences, 89* (2015), Mar., pp. 210-221
[5] Veljic, D. M., *et al.*, Experimental and Numerical Thermo-Mechanical Analysis of Friction Stir Welding of High-Strength Alluminium Alloy, *Thermal Science, 18* (2014), Suppl. 1, pp. S29-S38
[6] Lord, H., Shulman, Y., A Generalized Dynamical Theory of Thermoelasticity, *Journal of the Mechanics and Physics of Solids, 15* (1967), 5, pp. 299-309
[7] Beranek, M. W., *et al.*, Characterization of 63Sn37Pb and 80Au2OSn Solder Sealed Optical Fiber Feedthroughs Subjected to Repetitive Thermal Cycling, *IEEE Transactions on Advanced Packaging, 24* (2001), 4, pp. 576-585
[8] Luo, X., *et al.*, Thermal-Structural Coupling Analysis Based on ANSYS for Optical Feedthrough, *Proceedings*, The 5th International Conference on Advanced Design and Manufacturing Engineering (ICADME 2015), Shenzhen, China, 2015, pp. 2016-2021
[9] Chen, K. P., Development of Metal Oxide Nanostructure-Based Optical Sensors for Fossil Fuel Derived Gases Measurement at High Temperature, Final Technical Report, Department of Electrical and Computer Engineering, University of Pittsburgh, Pitsburg, Penn., USA, 2015
[10] Miller, D. L., Moshegov, N. T., All-Metal Ultrahigh Vacuum Optical Fiber Feedthrough, *Journal of Vacuum Science & Technology A, 19* (2001), 1, pp. 386-387
[11] Reinsch, T., Henninges, J., Temperature-Dependent Characterization of Optical Fibres for Distributed Temperature Sensing in Hot Geothermal Wells, *Measurement Science and Technology, 21* (2010), 9, 094022
[12] Reinsch, T., *et al.*, Simple Feed-Through for Coupling Optical Fibres into High Pressure and Temperature Systems, *Measurement Science and Technology, 24* (2013), 3, 037001
[13] Nowacki, W., *Thermoelasticity*, 2nd edition, Pergamon Press, PWN – Polish Scientific Publishers, 1986

Paper submitted: March 31, 2016
Paper revised: May 11, 2016
Paper accepted: May 13, 2016